

Quantum theory of multimode fields: Applications to optical resonators

C Viviescas and G Hackenbroich

Universität Duisburg–Essen, Fachbereich Physik, 45117 Essen, Germany

Abstract. A recently developed technique for the system–and–bath quantization of open optical cavities is applied to three resonator geometries: A one dimensional dielectric, a Fabry–Perot resonator, and a dielectric disk. The system–and–bath Hamiltonian for these geometries is derived starting from Maxwell’s equations and employed to compute the electromagnetic fields, the resonances, and the cavity gain factors. Exact agreement is found with standard quantization methods based on a modes–of–the–universe description. Our analysis provides a microscopic justification for the system–and–bath quantization even in the regime of spectrally overlapping modes. Combined with random–matrix theory our quantization method can serve as a starting point for a quantum theory of wave–chaotic and disordered optical media.

PACS numbers: 03.65.Yz, 42.50.-p, 42.50.Pq

1. Introduction

A standard description of losses in quantum mechanical systems is the system–and–bath model: One considers the system of interest coupled to a large quantum system acting as a reservoir or bath. The reservoir is assumed to be so large that its state is not much affected by the coupling to the system. In contrast, the coupling to the reservoir introduces both losses and noise for the system dynamics. In optical resonators the system–and–bath model has been used for more than 40 years [1, 2, 3] as a phenomenological description for the leakage of radiation into the external electromagnetic field.

In two recent papers [4, 5] we reported a *microscopic* derivation of the system–and–bath model from Maxwell’s equations and derived explicit expressions for the coupling amplitudes between system and bath modes. We demonstrated that the model not only applies to good resonators with spectrally well–separated modes but that it also provides an *exact* description for spectrally–overlapping or even overdamped modes. The field quantization in the presence of mode overlap has generated a substantial literature in recent years [6, 7, 8]. The motivation for our work came from recent studies of unstable optical cavities [9, 10, 11] and from experiments on strongly disordered amplifying media [12, 13, 14, 15], so-called random lasers. The losses in such lasers are typically much larger than in traditional lasers as the light is not confined by mirrors

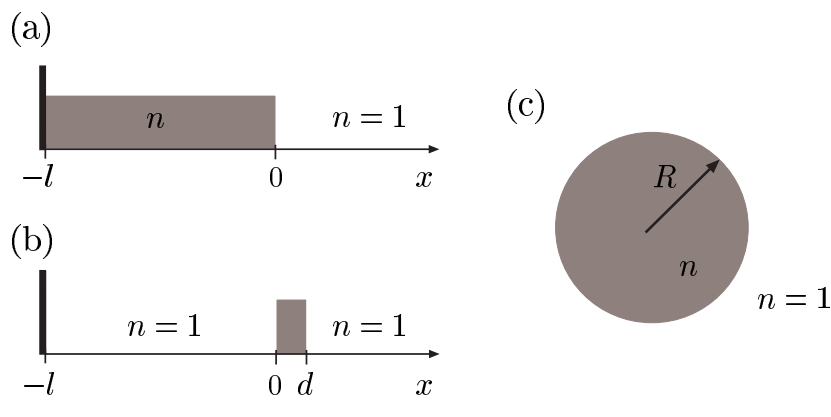


Figure 1. Open optical cavities studied in this paper: (a) A one-dimensional dielectric slab of length l with (positive) refractive index n bounded on one side ($x = -l$) by a perfectly reflecting mirror. (b) A one-dimensional cavity bounded by a perfectly reflecting mirror at ($x = -l$) and a thin semi-transparent mirror of width $d \ll l$ at ($x = 0$). (c) A two-dimensional dielectric disk with refractive index n .

but by the multiple chaotic scattering within the disordered medium. The amount of disorder determines both the laser mode amplitudes and frequencies. Therefore, the modes of random media depend on the statistical properties of the underlying random medium, and must be analyzed in a statistical fashion. Traditional methods of field-quantization, such as the so-called modes-of-the-universe approach [16], are not suited for a statistical description as they do not provide explicit information about the field inside the resonator region. In contrast, statistics naturally enters our system-and-bath model [4, 5] when the internal system dynamics is modeled by random-matrix theory [17]. In our previous work we have focused on the general derivation of the system-and-bath model, the discussion of the resulting system dynamics, and the connection with random-matrix theory. It is the purpose of the present paper to demonstrate our method explicitly for a number of models frequently used for optical resonators.

Specifically, we consider the three types of cavities shown in figure 1: (a) A one-dimensional dielectric slab with (positive) refractive index n bounded on one side by a perfectly reflecting mirror, (b) a one-dimensional cavity defined by a perfectly reflecting mirror on one side and a thin semi-transparent mirror on the other side, and (c) a two-dimensional dielectric disk with refractive index n . The dielectrics are embedded in empty space. The normal modes of all three systems in question as well as their scattering properties can be computed exactly. Likewise, exact expressions can be obtained for the electromagnetic fields both within the cavities and in the external region. This makes all three models an ideal testing ground for our system-and-bath description. According to that description the Hamiltonian of the complete system, comprising the resonator and the external region, can be represented as

$$H = \sum_{\lambda} \hbar\omega_{\lambda} a_{\lambda}^{\dagger} a_{\lambda} + \sum_m \int_{\omega_m}^{\infty} d\omega \hbar\omega b_m^{\dagger}(\omega) b_m(\omega)$$

$$+ \hbar \sum_{\lambda} \sum_m \int_{\omega_m}^{\infty} d\omega \left[\mathcal{W}_{\lambda m}(\omega) a_{\lambda}^{\dagger} b_m(\omega) + \mathcal{V}_{\lambda m}(\omega) a_{\lambda} b_m(\omega) + \text{H.c.} \right]. \quad (1)$$

There is a discrete set of cavity modes with index λ , and a continuous set of external modes labeled by the frequency ω and the discrete index m , which specifies the asymptotic boundary conditions far from the resonator (including polarization); ω_m is the frequency threshold above which external modes with the “channel”-index m exist. The operators a_{λ} and a_{λ}^{\dagger} are, respectively, the bosonic annihilation and creation operators associated with the cavity modes. They satisfy the standard commutation relations $[a_{\lambda}, a_{\lambda'}] = 0$, $[a_{\lambda}, a_{\lambda'}^{\dagger}] = \delta_{\lambda\lambda'}$. Likewise, the channel operators $b_m(\omega)$ and $b_m^{\dagger}(\omega)$ satisfy the commutation relations $[b_m(\omega), b_n(\omega')] = 0$, $[b_m(\omega), b_n^{\dagger}(\omega')] = \delta_{mn} \delta(\omega - \omega')$. Operators related to different subsystems commute. Explicit expressions for the coupling amplitudes $\mathcal{W}_{\lambda m}(\omega)$, $\mathcal{V}_{\lambda m}(\omega)$ will be given below.

The electric and magnetic fields are exactly represented within the system-and-bath approach by

$$\begin{aligned} \mathbf{E}(\mathbf{r}, t) = & i \sum_{\lambda} \left(\frac{\hbar\omega_{\lambda}}{2} \right)^{1/2} [a_{\lambda}(t) \mathbf{u}_{\lambda}(\mathbf{r}) - \text{H.c.}] \\ & + i \sum_m \int_{\omega_m}^{\infty} d\omega \left(\frac{\hbar\omega}{2} \right)^{1/2} [b_m(\omega, t) \mathbf{v}_m(\omega, \mathbf{r}) - \text{H.c.}], \end{aligned} \quad (2a)$$

$$\begin{aligned} \mathbf{B}(\mathbf{r}, t) = & c \sum_{\lambda} \left(\frac{\hbar}{2\omega_{\lambda}} \right)^{1/2} [a_{\lambda}(t) (\nabla \times \mathbf{u}_{\lambda})(\mathbf{r}) + \text{H.c.}] \\ & + c \sum_m \int_{\omega_m}^{\infty} d\omega \left(\frac{\hbar}{2\omega} \right)^{1/2} [b_m(\omega, t) (\nabla \times \mathbf{v}_m(\omega, \mathbf{r})) + \text{H.c.}], \end{aligned} \quad (2b)$$

where c is the velocity of light in vacuum. The modes $\mathbf{u}_{\lambda}(\mathbf{r})$ and $\mathbf{v}_m(\omega, \mathbf{r})$ have support only in the resonator and the external region, respectively. Although the expansions (2a) and (2b) reduce precisely to the standard expressions known from closed systems, the field *dynamics* given by Hamiltonian (1) is fundamentally different due to the coupling between the resonator and the external region [5, 18].

The microscopic formulation of the system-and-bath model must include a definition of the system modes \mathbf{u}_{λ} and the bath modes $\mathbf{v}_m(\omega)$. We will specify proper definitions below for the three systems of interest, but note at this point that these definitions (and the definition of the system-and-bath Hamiltonian itself) entail some degree of arbitrariness. This arbitrariness arises generically for open resonators; its origin is that the separation of space into two regions “inside” and “outside” the resonator is not unique. Consider for example a cavity with an opening, i.e. a hole in the material walls of the cavity boundary. Any choice of a fictitious surface covering the hole yields its own inside/outside separation. Moreover, different boundary conditions may be imposed at the chosen separating surface. Nevertheless, each such surface and boundary condition entail eigenmodes allowing to represent the electromagnetic field almost everywhere. We emphasize that the expansion cannot be expected to converge

uniformly or even pointwise, and in particular not on an arbitrarily chosen boundary. Still the system-and-bath representation is exact in the L^2 sense required by quantum mechanics. The freedom in the choice of the separating surface and the boundary conditions manifests itself in the Hamiltonian (1) and the field expansions (2a) and (2b): the internal frequencies ω_λ , the coupling amplitudes \mathcal{W} and \mathcal{V} , and the mode functions \mathbf{u} and \mathbf{v} , all depend explicitly on these choices. However, we show below that all physical observables, in particular the electromagnetic fields and the scattering amplitudes, do not rely on these choices and only depend on the physical boundary conditions imposed by Maxwell's equations.

The outline of the paper is as follows. In section 2 we collect the main results of our system-and-bath approach relevant for resonant cavities. In sections 3–5 the method is applied to the three resonators introduced earlier. We compute the respective system-and-bath Hamiltonians, and show that the electromagnetic fields and the scattering properties agree exactly with results obtained by direct solutions of the quantization problem. Performing the computations for different sets of boundary conditions along the surface separating the resonator and channel region, we demonstrate that the physical observables are independent of that choice of boundary condition. We conclude in section 6.

2. System-and-bath quantization

In two recent papers [4, 5] we developed a microscopic system-and-bath approach to the field quantization in open optical cavities. To keep the present paper self-contained we summarize the relevant results in the present section. Our quantization technique applies to linear dielectric media characterized by a scalar dielectric constant $\epsilon(\mathbf{r})$ that may explicitly depend on position and that we assume real and frequency independent. Working in the Coulomb gauge in the absence of charges, the exact eigenmodes $\mathbf{f}_m(\omega, \mathbf{r})$ of Maxwell's equations [19] are solutions of the Helmholtz equation

$$\nabla \times [\nabla \times \mathbf{f}_m(\omega, \mathbf{r})] - \frac{\epsilon(\mathbf{r})\omega^2}{c^2} \mathbf{f}_m(\omega, \mathbf{r}) = \mathbf{0}, \quad (3)$$

and satisfy the generalized transversality condition $\nabla \cdot [\epsilon(\mathbf{r})\mathbf{f}_m(\omega, \mathbf{r})] = 0$. The modes are labeled by the continuous frequency ω and a discrete index m ; the latter specifies the asymptotic conditions far away from the resonator. For example, these conditions could correspond to a scattering problem with incoming and outgoing waves. Then $\mathbf{f}_m(\omega, \mathbf{r})$ represents a solution with an incoming wave only in channel m and outgoing waves in all scattering channels. Using notation from scattering theory, the region outside the resonator will be called channel region below. We follow reference [19] and stick to the usual internal product with respect to which the differential operator in equation (3) is not Hermitian. However, the substitution

$$\mathbf{f}_m(\omega, \mathbf{r}) = \frac{1}{\sqrt{\epsilon(\mathbf{r})}} \boldsymbol{\phi}_m(\omega, \mathbf{r}) \quad (4)$$

transforms equation (3) into the hermitian eigenvalue problem

$$L\phi_m(\omega, \mathbf{r}) \equiv \frac{1}{\sqrt{\epsilon(\mathbf{r})}} \nabla \times \left(\nabla \times \frac{\phi_m(\omega, \mathbf{r})}{\sqrt{\epsilon(\mathbf{r})}} \right) = \frac{\omega^2}{c^2} \phi_m(\omega, \mathbf{r}), \quad (5)$$

for the operator L . The functions $\phi_m(\omega)$ provide a complete orthonormal set in the space of L^2 functions. It follows from equation (4) that the functions $\mathbf{f}_m(\omega)$ satisfy the orthonormalization condition

$$\int d\mathbf{r} \epsilon(\mathbf{r}) \mathbf{f}_m(\omega, \mathbf{r}) \mathbf{f}_n(\omega', \mathbf{r}) = \delta_{mn} \delta(\omega - \omega'). \quad (6)$$

The quantization of the electromagnetic field in terms of eigenmodes of the Helmholtz equation is known as the modes-of-the-universe approach [16, 20, 19]. Within this approach the field Hamiltonian reduces to a sum of independent harmonic oscillators

$$H = \frac{1}{2} \sum_m \int_{\omega_m}^{\infty} d\omega \hbar \omega \left(A_m^\dagger(\omega) A_m(\omega) + A_m(\omega) A_m^\dagger(\omega) \right), \quad (7)$$

and the electromagnetic fields take the standard form

$$\mathbf{E} = i \sum_m \int_{\omega_m}^{\infty} d\omega \left(\frac{\hbar \omega}{2} \right)^{1/2} \left[A_m(\omega) e^{-i\omega t} \mathbf{f}_m(\omega, \mathbf{r}) - \text{H.c.} \right], \quad (8a)$$

$$\mathbf{B} = c \sum_m \int_{\omega_m}^{\infty} d\omega \left(\frac{\hbar}{2\omega} \right)^{1/2} \left[A_m(\omega) e^{-i\omega t} (\nabla \times \mathbf{f}_m(\omega, \mathbf{r})) + \text{H.c.} \right]. \quad (8b)$$

The fundamental disadvantage of the modes-of-the-universe approach is that it makes no distinction between the cavity and the external region. As a consequence, the method fails to single out explicit information about the field inside the cavity.

The system-and-bath technique is based on the separation of the electromagnetic fields into an inside and an outside contribution. Likewise, the eigenmodes of the Helmholtz equation are decomposed into contributions ‘‘living’’ inside the resonator or in the channel space. At a formal level one can achieve the inside/outside separation by introducing the projection operators [21, 5]

$$\mathcal{Q} = \int_{\mathbf{r} \in I} d\mathbf{r} |\mathbf{r}\rangle \langle \mathbf{r}| \quad \text{and} \quad \mathcal{P} = \int_{\mathbf{r} \notin I} d\mathbf{r} |\mathbf{r}\rangle \langle \mathbf{r}|, \quad (9)$$

where $|\mathbf{r}\rangle$ denotes a standard position eigenket and I represents the resonator region. The projection operators are orthogonal, $\mathcal{Q}\mathcal{P} = \mathcal{P}\mathcal{Q} = 0$, and complete, $\mathcal{Q} + \mathcal{P} = 1$. Thus an arbitrary function ϕ in Hilbert space may be decomposed into its projections onto the resonator and channel space

$$|\phi\rangle = \mathcal{Q}|\phi\rangle + \mathcal{P}|\phi\rangle \equiv |\mu\rangle + |\nu\rangle. \quad (10)$$

Acting on $|\phi\rangle$ with the operator L we obtain

$$L|\phi\rangle = L_{\mathcal{Q}\mathcal{Q}}|\mu\rangle + L_{\mathcal{Q}\mathcal{P}}|\nu\rangle + L_{\mathcal{P}\mathcal{Q}}|\mu\rangle + L_{\mathcal{P}\mathcal{P}}|\nu\rangle, \quad (11)$$

where $L_{\mathcal{Q}\mathcal{Q}}$ and $L_{\mathcal{P}\mathcal{P}}$ are the projections of L onto the resonator and channel space, and $L_{\mathcal{Q}\mathcal{P}}$ and $L_{\mathcal{P}\mathcal{Q}}$ the coupling terms. As explained in the introduction and illustrated

in references [5, 22], this decomposition is by no means unique: different choices of the separating surface and different boundary conditions along that surface result in different decompositions of L . However, all those decompositions are subject to the condition that L remains Hermitian, i.e. $L_{\mathcal{Q}\mathcal{Q}} = L_{\mathcal{Q}\mathcal{Q}}^\dagger$, $L_{\mathcal{P}\mathcal{P}} = L_{\mathcal{P}\mathcal{P}}^\dagger$ and $L_{\mathcal{Q}\mathcal{P}} = L_{\mathcal{P}\mathcal{Q}}^\dagger$.

The projections $L_{\mathcal{Q}\mathcal{Q}}$ and $L_{\mathcal{P}\mathcal{P}}$ define Hermitian eigenvalue problems for the isolated cavity and channel region, respectively. The closed resonator modes $|\boldsymbol{\mu}_\lambda\rangle$ are the solutions of the eigenvalue problem

$$L_{\mathcal{Q}\mathcal{Q}}|\boldsymbol{\mu}_\lambda\rangle = \left(\frac{\omega_\lambda}{c}\right)^2 |\boldsymbol{\mu}_\lambda\rangle, \quad (12)$$

and form a discrete orthonormal basis for the cavity subspace. Likewise, the channels modes $|\boldsymbol{\nu}_m(\omega)\rangle$ satisfy the equation

$$L_{\mathcal{P}\mathcal{P}}|\boldsymbol{\nu}_m(\omega)\rangle = \left(\frac{\omega}{c}\right)^2 |\boldsymbol{\nu}_m(\omega)\rangle, \quad (13)$$

and constitute a continuous basis for the channel region. We note that the functions $\boldsymbol{\mu}_\lambda(\mathbf{r})$ have support only inside the resonator, while the functions $\boldsymbol{\nu}_m(\omega, \mathbf{r})$ are nonzero only in the channel region.

It follows from these definitions that the resonator and channel modes form a complete set of Hilbert space functions in the respective subregions. One may therefore use these functions to expand the eigenstates of the Helmholtz equation

$$\boldsymbol{\phi}_m(\omega, \mathbf{r}) = \sum_\lambda \alpha_{m\lambda}(\omega) \boldsymbol{\mu}_\lambda(\mathbf{r}) + \sum_{m'} \int_{\omega_{m'}}^{\infty} d\omega' \beta_{mm'}(\omega, \omega') \boldsymbol{\nu}_{m'}(\omega', \mathbf{r}), \quad (14a)$$

$$\mathbf{f}_m(\omega, \mathbf{r}) = \sum_\lambda \alpha_{m\lambda}(\omega) \mathbf{u}_\lambda(\mathbf{r}) + \sum_{m'} \int_{\omega_{m'}}^{\infty} d\omega' \beta_{mm'}(\omega, \omega') \mathbf{v}_{m'}(\omega', \mathbf{r}), \quad (14b)$$

where we introduced the functions $\mathbf{u}_\lambda(\mathbf{r}) \equiv \boldsymbol{\mu}_\lambda(\mathbf{r})/\sqrt{\epsilon(\mathbf{r})}$ and $\mathbf{v}_m(\omega, \mathbf{r}) \equiv \boldsymbol{\nu}_m(\omega, \mathbf{r})/\sqrt{\epsilon(\mathbf{r})}$. The expansion coefficients can be recovered from the mode functions using the relations

$$\alpha_{m\lambda}(\omega) = \langle \boldsymbol{\mu}_\lambda | \boldsymbol{\phi}_m(\omega) \rangle, \quad (15a)$$

$$\beta_{mm'}(\omega, \omega') = \langle \boldsymbol{\nu}_{m'}(\omega') | \boldsymbol{\phi}_m(\omega) \rangle. \quad (15b)$$

The system–and–bath Hamiltonian (1) and the field representations (2a) and (2b) follow upon the introduction of bosonic creation and annihilation operators a and a^\dagger for the cavity modes, and similar operators b and b^\dagger for the channel modes. Finally, the coupling amplitudes in the Hamiltonian (1) are of the form

$$\mathcal{W}_{\lambda m}(\omega) = \frac{c^2}{2\sqrt{\omega_\lambda\omega}} \langle \boldsymbol{\mu}_\lambda | L_{\mathcal{Q}\mathcal{P}} | \boldsymbol{\nu}_m(\omega) \rangle, \quad (16a)$$

$$\mathcal{V}_{\lambda m}(\omega) = \frac{c^2}{2\sqrt{\omega_\lambda\omega}} \langle \boldsymbol{\mu}_\lambda^* | L_{\mathcal{Q}\mathcal{P}} | \boldsymbol{\nu}_m(\omega) \rangle. \quad (16b)$$

The notation $|\boldsymbol{\mu}^*\rangle$ means $\langle \mathbf{r} | \boldsymbol{\mu}^* \rangle \equiv \boldsymbol{\mu}^*(\mathbf{r})$. For time reversal invariant systems the wave functions may be chosen real, then the amplitudes \mathcal{W} and \mathcal{V} become real and identical, $\mathcal{W} = \mathcal{V}$.

In order to test the system–and–bath approach for the resonators of interest we compute several physical observables below. Examples include the electromagnetic fields, and the eigenmodes of the Helmholtz equation. We also study the cavity resonances, i.e. the complex frequencies that determine the cavity response to external excitations in the presence of the coupling to the outside world. Formally the resonances are found as the poles of the resolvent operator $\mathcal{G}(\omega)$ projected onto the cavity space and analytically continued in the second Riemann sheet [23]. After projection the resolvent can be written as

$$\mathcal{G}_{QQ}(\omega) = \frac{1}{\left(\frac{\omega}{c}\right)^2 - L_{\text{eff}}(\omega)}, \quad (17)$$

where the non-Hermitian operator $L_{\text{eff}}(\omega)$ is expressed through the projections of the differential operator L ,

$$\begin{aligned} L_{\text{eff}}(\omega) &\equiv L_{QQ} + L_{QP} \frac{1}{\left(\frac{\omega}{c}\right)^2 - L_{PP} + i\epsilon} L_{PQ}, \\ &= L_{QQ} + c^2 L_{QP} \sum_m \int_{\omega_m}^{\infty} d\omega' \frac{|\boldsymbol{\nu}_m(\omega')\rangle \langle \boldsymbol{\nu}_m(\omega')|}{\omega^2 - \omega'^2 + i\epsilon} L_{PQ}, \end{aligned} \quad (18)$$

here the limit $\epsilon \rightarrow 0^+$ is implied. The second line follows upon using the completeness of the channels modes with the help of equation (13). The operator $L_{\text{eff}}(\omega)$ is closely related to the effective Hamiltonian in open quantum systems [22]. To determine the system resonances one must solve the eigenvalue problem,

$$L_{\text{eff}}(\omega)|\xi_i(\omega)\rangle = \sigma_i^2(\omega)|\xi_i(\omega)\rangle. \quad (19)$$

Since $L_{\text{eff}}(\omega)$ depends parametrically on ω , both its right eigenstates $|\xi_i(\omega)\rangle$ and the complex eigenvalues $\sigma_i(\omega)$ generally depend on ω as well. The states $|\xi_i(\omega)\rangle$ correspond to the Kapur–Peierls states [24, 25] of scattering theory. Combining equations (17) and (19) the cavity resonances are found as the solutions of the fixed point equation $c\sigma_i(\omega) = \omega$. We show below that this resonance condition is independent of the inside/outside separation and the choice of boundary condition made within the system–and–bath description.

A well-known quantity that shows resonant behavior is the cavity gain factor

$$G^c(\omega) = \frac{\int_{\mathbf{r} \in I} d\mathbf{r} \rho(\omega, \mathbf{r})}{\int_{\mathbf{r} \in I} d\mathbf{r} \rho_0(\omega, \mathbf{r})}, \quad (20)$$

that is closely related to the dwell time of scattered radiation inside the resonator [26]. Here, $\rho(\omega, \mathbf{r})$ is the local density of states inside the cavity and $\rho_0(\omega, \mathbf{r})$ the free space local density of states in the absence of the cavity. The cavity gain factor thus measures the change in the local density of states introduced by the cavity. For later use we note that the integrated density of states can be expressed in terms of the expansions coefficients (15a),

$$\int_{\mathbf{r} \in I} d\mathbf{r} \rho(\omega, \mathbf{r}) = \sum_m \sum_{\lambda} |\alpha_{m\lambda}(\omega)|^2. \quad (21)$$

3. One dimensional dielectric cavity

Our first example is the one dimensional dielectric cavity depicted in figure 1(a) [27]. The dielectric with refractive index n is nonabsorbing and nondispersive. It is bounded by a perfectly reflecting mirror at $x = -l$ while there is no mirror at the other end of the dielectric at $x = 0$. The free space outside the cavity runs from $x = 0$ to infinity, and light propagates freely there, $n = 1$. We assume the electromagnetic field to be linearly polarized with the electric field vector pointing in the z -direction. Cavity field excitations will decay due to leakage into the empty half-space. The dielectric function of the total system including the cavity and the attached half-space is given by

$$\epsilon(x) = n^2\Theta(-x) + \Theta(x), \quad (22)$$

where the Heavyside-function $\Theta(x)$ is equal to one for positive x and vanishes for negative x . The exact eigenmodes of Maxwell's equations for this problem are given in equation (A.1). To solve the problem within the system-and-bath approach, we separate system and bath at $x = 0$. The cavity thus runs from $x = -l$ to $x = 0$, and the channel region from $x = 0$ to ∞ . The boundary conditions at the interface are only restricted by the requirement that they lead to an Hermitian eigenvalue problem. Below we address two different such boundary conditions: In the first case we set Neumann boundary conditions for the cavity; Hermiticity [22, 5] then imposes Dirichlet conditions for the channel problem. In the second case we consider the inverse situation with Dirichlet boundary condition for the cavity and Neumann conditions outside.

3.1. Cavity with von-Neumann boundary conditions

The inside/outside decomposition of the differential operator L reads [5]

$$L_{\mathcal{Q}\mathcal{Q}}\mu(x) = -\frac{1}{n^2}\frac{d^2}{dx^2}\mu(x) + \frac{\delta(x-0_-)}{n^2}\frac{d}{dx'}\mu(x')\Big|_{x'=0_-}, \quad (23a)$$

$$L_{\mathcal{P}\mathcal{P}}\nu(x) = -\frac{d^2}{dx^2}\nu(x) - \delta'(x-0_+)\nu(0_+), \quad (23b)$$

$$L_{\mathcal{P}\mathcal{Q}}\mu(x) = \frac{\delta'(x-0_+)}{n}\mu(0_-), \quad (23c)$$

$$L_{\mathcal{Q}\mathcal{P}}\nu(x) = -\frac{\delta(x-0_-)}{n}\frac{d}{dx'}\nu(x')\Big|_{x'=0_+}. \quad (23d)$$

The shorthands 0_{\mp} indicate the limits where the interface at $x = 0$ is approached from inside respectively outside the resonator. The singular terms guarantee the matching conditions for the electromagnetic field at the interface. In addition, these terms ensure the Hermiticity of $L_{\mathcal{Q}\mathcal{Q}}$ and $L_{\mathcal{P}\mathcal{P}}$. The range of the operators in equations (23a) and (23b) within Hilbert space is given by the functions for which the singular term vanishes.

The eigenmodes $\mu_{\lambda}(x)$ of the closed cavity are the solutions of the eigenvalue problem $L_{\mathcal{Q}\mathcal{Q}}\mu_{\lambda}(x) = k_{\lambda}^2\mu_{\lambda}(x)$ with $k_{\lambda} = \omega_{\lambda}/c$. From equation (23a), they satisfy the equation

$$\frac{d^2}{dx^2}\mu_{\lambda}(x) + n^2k_{\lambda}^2\mu_{\lambda}(x) = 0, \quad (24)$$

subject to the boundary conditions

$$\mu_\lambda(-l) = 0, \quad (25a)$$

$$\left. \frac{d}{dx} \mu_\lambda(x) \right|_{x=0_-} = 0. \quad (25b)$$

The first condition is imposed by the perfectly reflecting mirror at $x = -l$, and the second follows from the requirement that the singular boundary term applied to μ_λ must vanish. The normalized solutions of the eigenvalue problem form the discrete set

$$\mu_\lambda(x) = \sqrt{\frac{2}{l}} \sin(nk_\lambda(x+l)), \quad (26)$$

with wave numbers $k_\lambda = (2\lambda + 1)\pi/2nl$ ($\lambda = 0, 1, 2, \dots$). In the channel region, the eigenvalue problem reads

$$\frac{d^2}{dx^2} \nu(k, x) + k^2 \nu(k, x) = 0, \quad (k = \omega/c), \quad (27)$$

with Dirichlet conditions at the resonator surface,

$$\nu(k, 0_+) = 0. \quad (28)$$

This determines a continuous set of δ -normalized channel modes,

$$\nu(k, x) = \sqrt{\frac{2}{\pi}} \sin(kx). \quad (29)$$

Since both the cavity and channel modes are real valued functions, the coupling amplitudes \mathcal{W} and \mathcal{V} become real and identical, $\mathcal{W} = \mathcal{V}$. Combining equations (16a), (23d) with the mode functions (26) and (29), we obtain

$$\mathcal{W}_\lambda(k) = \mathcal{V}_\lambda(k) = \frac{(-1)^{\lambda+1}}{n} \sqrt{\frac{k}{\pi k_\lambda l}}. \quad (30)$$

The result for the internal frequencies $\omega_\lambda = ck_\lambda$, together with the coupling amplitudes (30), and the mode functions (26) and (29), completely specify the system-and-bath Hamiltonian and the electric and magnetic field.

We now turn to an illustration of our results. To compare the exact scattering states with their representation in terms of cavity and channel modes, we combine equations (15a), (15b) with the results (A.1), (26), and (29). This yields the expansion coefficients

$$\alpha_\lambda(k) = \frac{(-1)^{\lambda+1} I_k k \cos(nkl)}{n\sqrt{\pi l}(k^2 - k_\lambda^2)}, \quad (31)$$

$$\beta(k, k') = \frac{1}{2\pi} \left[\mathcal{P} \left(\frac{2k'(1+S_k)}{k'^2 - k^2} \right) - i\pi(1 - S_k)\delta(k' - k) \right]. \quad (32)$$

The symbol \mathcal{P} denotes the principal value. The S-matrix S_k and the amplitude I_k are given, respectively, by equations (A.2) and (A.3). Figure 2 shows the real part of the scattering wave function with wavenumber $kl = 18$. We compare the exact result (solid gray line) with the system-and-bath expansion (dashed line). In the resonator region we only included 11 cavity modes with wavenumber centered around $kl = 18$. The agreement is very good; deviations are only visible close to $x = 0$, i.e. near the

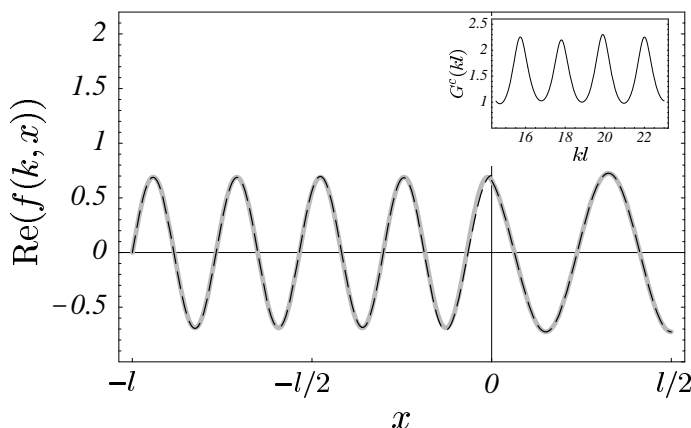


Figure 2. Real part of the scattering wave function corresponding to $kl = 18$, computed for a one dimensional dielectric cavity with refractive index $n = 1.5$. The solid line is the exact solution, the dashed line the expansion in terms of the resonator and channels modes. Only 11 cavity modes with $k_\lambda l$ around $kl = 18$ were included. The inset shows the cavity gain factor as function of kl for a range around $kl = 18$.

boundary separating system and bath. It has been argued before [28] that cavity or channel expansions must fail close to the boundary; so a remark concerning the status of such expansions is in order here: The inclusion of all cavity and all channel modes yields an exact point-to-point representation of the scattering function and its derivative, everywhere *except* for the point $x = 0$. This representation does not converge uniformly but it is exact in the L^2 sense. Therefore the system-and-bath expansion is an exact representation of the scattering state in the underlying Hilbert space.

To determine the cavity resonances we solve the eigenvalue problem for the non-Hermitian operator $L_{\text{eff}}(k)$. Explicit calculation (Appendix B) shows that $L_{\text{eff}}(k)$ acts on an arbitrary resonator state $\mu(x)$ according to

$$L_{\text{eff}}(k)\mu(x) = -\frac{1}{n^2} \frac{d^2}{dx^2} \mu(x) + \frac{\delta(x-0_-)}{n^2} \left[\frac{d}{dx'} \mu(x') \Big|_{x'=0_-} - ik\mu(0_-) \right]. \quad (33)$$

Due to the singular term, the action of $L_{\text{eff}}(k)$ generally goes beyond Hilbert space. The range of $L_{\text{eff}}(k)$ within Hilbert space is defined by the wave functions for which the singular term vanishes. It follows that the right eigenstates $\xi_j(k, x)$ are solutions of the Helmholtz equation

$$\frac{d^2}{dx^2} \xi_j(k, x) + n^2 \sigma_j^2(k) \xi_j(k, x) = 0, \quad (34)$$

that obey the boundary conditions

$$\xi_j(k, -l) = 0, \quad (35a)$$

$$\frac{d}{dx'} \xi_j(k, x') \Big|_{x'=0_-} = ik \xi_j(k, 0_-). \quad (35b)$$

The first condition results from the perfect mirror at $x = -l$ while the second defines the so-called Siegert boundary condition. It accounts for the leakage out of the cavity:

In the channel region that boundary condition implies a purely outgoing wave. For a fixed value of k , one finds the discrete set of solutions

$$\xi_j(k, x) = A_j(k) \sin(n\sigma_j(k)(x + l)), \quad (36)$$

with some normalization factors $A_j(k)$. Substituting the solutions into equation (35b) we obtain the secular equation for the eigenvalues,

$$\sigma_j(k) = \frac{i}{n} k \tan(n\sigma_j(k)l). \quad (37)$$

The fixed point equation $k = \sigma_j(k)$ determines the cavity resonances. Analytical continuation of equation (37) into the complex plane then yields the resonance condition

$$\tan(nkl) + in = 0, \quad (38)$$

which has solutions only for complex k . The resonances can be found analytically and are given by

$$k_j = \frac{1}{nl} \begin{cases} \frac{(2j+1)\pi}{2} + \frac{i}{2} \ln(|r|); & j = 0, 1, \dots & (n > 1), \\ j\pi + \frac{i}{2} \ln(|r|); & j = 1, 2, \dots & (n < 1), \end{cases} \quad (39)$$

where $r = (n-1)/(n+1)$ is the reflection amplitude at the dielectric surface. Comparison with the direct calculation (cf. equation (A.2)) shows that the resonances coincide with the poles of the scattering-matrix. All resonances have the same width and are located along a straight line in the lower half of the complex plane. The resonance spacing, i.e. the difference in real parts of two successive resonances, is constant, $\Delta = \pi/nl$. The resonances start to overlap when the modulus of the reflection amplitude becomes smaller than $|r| = \exp(-\pi)$.

We finally evaluate the cavity gain factor. The free-space local density of states is $\rho_0(k, x) = \sqrt{\frac{2}{\pi}} \sin^2(k(x+l))$. Integration over the cavity volume yields

$$\int_{-l}^0 dx \rho_0(k, x) = \frac{l}{\pi} \left[1 - \frac{\sin(2kl)}{2kl} \right]. \quad (40)$$

The integrated cavity density of states follows from equations (21) and (31) by means of the Poisson sum rule,

$$\begin{aligned} \int_{-l}^0 dx \rho(k, x) &= \frac{|I_k|^2 k^2 \cos^2(nkl)}{\pi l n^2} \sum_{\lambda=0}^{+\infty} \frac{1}{(k^2 - k_\lambda^2)^2} \\ &= \frac{l |I_k|^2}{4\pi} \left[1 - \frac{\sin(2nkl)}{2nkl} \right]. \end{aligned} \quad (41)$$

Combining these results with equation (A.3) for I_k , we obtain the cavity gain factor

$$G^c(k) = \frac{n^2 \left[1 - \frac{\sin(2nkl)}{2nkl} \right]}{\left[n^2 \cos^2(nkl) + \sin^2(nkl) \right] \left[1 - \frac{\sin(2kl)}{2kl} \right]}. \quad (42)$$

The inset in figure 2 shows the cavity gain factor over a range of kl . The peaks are equally spaced and have approximately the same high and width as expected from equation (39).

3.2. Cavity with Dirichlet boundary conditions

It is interesting to carry out the system–and–bath quantization in a basis other than that considered in the previous section. To that end we reconsider the dielectric resonator of figure 1(a) but perform the system–and–bath quantization with *interchanged* boundary conditions at the resonator/channel interface: The resonator modes are now required to satisfy Dirichlet boundary conditions at $x = 0$ while Neumann conditions hold for the channel modes. The differential operators corresponding to this choice have the form

$$L_{\mathcal{Q}\mathcal{Q}}\mu(x) = -\frac{1}{n^2} \frac{d^2}{dx^2} \mu(x) + \frac{\delta'(x - 0_-)}{n^2} \mu(0_-), \quad (43a)$$

$$L_{\mathcal{P}\mathcal{P}}\nu(x) = -\frac{d^2}{dx^2} \nu(x) - \delta(x - 0_+) \frac{d}{dx'} \nu(x') \Big|_{x'=0_+}, \quad (43b)$$

$$L_{\mathcal{P}\mathcal{Q}}\mu(x) = \frac{\delta(x - 0_+)}{n} \frac{d}{dx'} \mu(x') \Big|_{x'=0_-}, \quad (43c)$$

$$L_{\mathcal{Q}\mathcal{P}}\nu(x) = -\frac{\delta'(x - 0_-)}{n} \nu(0_+). \quad (43d)$$

The closed cavity eigenmodes of $L_{\mathcal{Q}\mathcal{Q}}$ solve the Helmholtz equation and satisfy Dirichlet boundary conditions both at $x = l$ and $x = 0_-$. The second of these conditions follows from the requirement that the application of $L_{\mathcal{Q}\mathcal{Q}}$ on any eigenmode must yield a vanishing singular contribution. The eigenmodes form the discrete set of functions

$$\mu_\lambda(x) = \sqrt{\frac{2}{l}} \sin(nk_\lambda(x + l)), \quad (44)$$

with eigenvalues $k_\lambda = \pi\lambda/nl$ ($\lambda = 1, 2, \dots$). In a similar fashion one finds the continuous set of channel modes

$$\nu(k, x) = \sqrt{\frac{2}{\pi}} \cos(kx), \quad (45)$$

that satisfy Neumann boundary conditions at $x = 0_+$. Substituting the mode functions into the definitions (16a) and (16b) we obtain the coupling amplitudes

$$\mathcal{W}_{\lambda k} = \mathcal{V}_{\lambda k} = (-1)^\lambda \sqrt{\frac{k_\lambda}{\pi k l}}. \quad (46)$$

We note that the cavity eigenfrequencies and the coupling amplitudes obtained with the present set of boundary conditions differ from the results obtained in the previous section. Consequently, two different system–and–bath Hamiltonians are obtained in the two cases. However, as we show below both Hamiltonians provide an equivalent, and exact, description of the field dynamics.

Expanding the modes–of–the–universe $f(k, x)$ in terms of resonator and channel modes, we find the expansions coefficients

$$\alpha_\lambda(k) = \frac{(-1)^\lambda I_k k_\lambda \sin(nkl)}{n\sqrt{\pi l}(k^2 - k_\lambda^2)}, \quad (47)$$

$$\beta(k, k') = \frac{i}{2\pi} \left[\mathcal{P} \left(\frac{2k(1 - S_k)}{k'^2 - k^2} \right) - i\pi(1 + S_k)\delta(k' - k) \right], \quad (48)$$

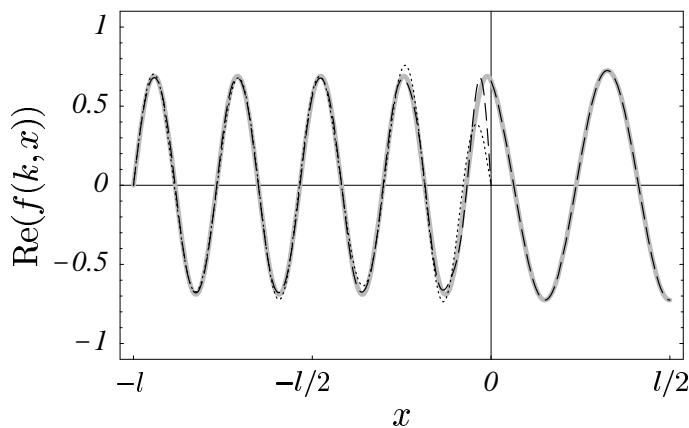


Figure 3. Real part of the scattering wave function for a one dimensional dielectric cavity with the same parameters as in figure 2. The solid gray curve is the exact solution. The system-and-bath expansion (dotted, dashed line) is based on 11, respectively, 25 cavity modes satisfying Dirichlet boundary conditions at $x = 0$. The dashed line for $x > 0$ is the representation in terms of channel modes.

with S_k and I_k defined, respectively, by equations (A.2) and (A.3). In figure 3 we compare the exact scattering wave function (A.1) (solid gray line) with the mode expansion in terms of the expansion coefficients (47) and (48). Perfect agreement is found in the channel region $x > 0$. In the cavity region there is slow convergence close to $x = 0$, due to the Dirichlet boundary conditions at $x = 0_-$. The slower convergence visible in figure 3 must be compared with the faster convergence found for the other set of boundary conditions (Figure 2). It indicates that, in spite of the freedom inherent in the projection formalism for the choice of boundary conditions, certain boundary conditions are better suited for the problem yielding good approximations with less terms in the mode expansions.

As in section 3.1 we can now evaluate the system resonances and the cavity gain factor. With the present boundary conditions the operator $L_{\text{eff}}(k)$ reduces to (see Appendix B)

$$L_{\text{eff}}(k)\mu(x) = -\frac{1}{n^2} \frac{d^2}{dx^2} \mu(x) + \frac{\delta'(x - 0_-)}{n^2} \left[\mu(0_-) + \frac{i}{k} \frac{d}{dx} \mu(x') \Big|_{x'=0_-} \right]. \quad (49)$$

It is illustrative to compare this with the result (33) that holds for interchanged resonator/channel boundary conditions. Both results differ in their singular terms. However, upon projection onto the Hilbert space the same operator is recovered as the singular contributions vanish. In both cases the resulting boundary condition at the resonator/channel-interface is the Siegert condition (35b).

The integrated cavity density of states follows upon combination of equations (21) and (47), with the result

$$\int_{-l}^0 dx \rho(k, x) = \frac{l|I_k|^2}{4\pi} \left[1 - \frac{\sin(2nkl)}{2nkl} \right]. \quad (50)$$

It agrees with the result (41) obtained for the other set of boundary conditions. This demonstrates that the physical observables are indeed independent of the choice of boundary conditions.

4. One dimensional cavity with a semitransparent mirror

The model of Ley and Loudon [29] is a one dimensional cavity defined by a totally reflecting mirror at one end and a semitransparent mirror at the other end (Figure 1(b)). The electric field is linearly polarized in the z -direction. Radiation can leak out through the semitransparent mirror modeled by a dielectric slab of width d and refractive index n . The limit $d \rightarrow 0$ and $n \rightarrow \infty$ with $n^2 d = \eta$ fixed is taken at the end of the calculation, here η is a factor characterizing the mirror transparency. In this limit, the frequency dependent mirror reflection and transmission amplitudes are given by

$$r(k) = \frac{ik\eta}{2 - ik\eta}, \quad t(k) = \frac{2}{2 - ik\eta}. \quad (51)$$

They obey the common relations for symmetric mirrors, $|r|^2 + |t|^2 = 1$ and $rt^* + r^*t = 0$.

The exact eigenmodes of Maxwell's equations for this problem are given in equation (A.4). Within the system-and-bath approach there are two natural ways of a resonator/channel separation: Either one assumes the mirror to be part of the cavity or the mirror is part of the channel region. Here, we stick to the latter choice. Accordingly, the cavity runs from $x = -l$ to $x = 0$ and the channel region from $x = 0$ to ∞ . The alternative definition with the mirror being part of the cavity can easily be shown to lead to the same physical results. We choose Dirichlet conditions for the resonator boundary at $x = 0_-$, which implies von Neumann conditions for the outside problem. The differential operators corresponding to these definitions are

$$L_{\mathcal{Q}\mathcal{Q}}\mu(x) = -\frac{d^2}{dx^2}\mu(x) + \delta'(x - 0_-)\mu(0_-), \quad (52a)$$

$$L_{\mathcal{P}\mathcal{P}}\nu(x) = -\frac{1}{n(x)}\frac{d^2}{dx^2}\left(\frac{\nu(x)}{n(x)}\right) - \frac{\delta(x - 0_+)}{n(x)}\frac{d}{dx'}\left(\frac{\nu(x')}{n(x')}\right)\Big|_{x'=0_+}, \quad (52b)$$

$$L_{\mathcal{P}\mathcal{Q}}\mu(x) = \frac{\delta(x - 0_+)}{n(x)}\frac{d}{dx'}\mu(x')\Big|_{x'=0_-}, \quad (52c)$$

$$L_{\mathcal{Q}\mathcal{P}}\nu(x) = -\delta'(x - 0_-)\frac{\nu(0_+)}{n(0_+)}, \quad (52d)$$

where $n(x)$ is the refractive index in the channel region,

$$n(x) = \begin{cases} n & (0_+ \leq x \leq d), \\ 1 & (d < x). \end{cases} \quad (53)$$

The eigenvalue problem defined by $L_{\mathcal{Q}\mathcal{Q}}$ reduces to that of the dielectric resonator of section 3.2 in the case when the dielectric function equals 1. Adopting our earlier results in that limiting case we find the closed cavity eigenmodes

$$\mu_\lambda(x) = \sqrt{\frac{2}{l}} \sin(k_\lambda(x + L)), \quad (54)$$

with the eigenvalues $k_\lambda = \pi\lambda/l$ ($\lambda = 1, 2, \dots$). The channel modes are the solutions of the Helmholtz equation

$$\frac{d^2}{dx^2}\nu(k, x) + n^2(x)k^2\nu(k, x) = 0, \quad (55)$$

with Neumann boundary conditions at $x = 0_+$. In addition, they must satisfy the two conditions

$$\frac{1}{n}\nu(k, d_-) = \nu(k, d_+), \quad (56)$$

$$\frac{1}{n}\frac{d}{dx}\nu(k, x)\Big|_{x=d_-} = \frac{d}{dx}\nu(k, x)\Big|_{x=d_+}, \quad (57)$$

imposed by the continuity of the electric and magnetic field at the right end of the semitransparent mirror. The shorthands d_\pm indicate the limit where d is approached from the left (d_-) or from the right (d_+). Solving for $\nu(k, x)$ and taking the limit $d \rightarrow 0$, $n \rightarrow \infty$ with $n^2d = \eta$, one obtains the following continuous set of channel modes,

$$\nu(k, x) = \frac{1}{\sqrt{2\pi}}(e^{-ikx} + S_c(k)e^{ikx}), \quad S_c(k) = \frac{i - \eta k}{i + \eta k}. \quad (58)$$

The coupling amplitudes follow upon substituting the wavefunctions (54), (58) into the definitions (16a) and (16b). The result is

$$\mathcal{W}_\lambda(k) = \mathcal{V}_\lambda(k) = \frac{(-1)^\lambda}{1 - i\eta k} \sqrt{\frac{k_\lambda}{\pi k l}}. \quad (59)$$

Finally, the representation of the exact modes $f(k, x)$ in terms of the system and bath modes yields the expansion coefficients

$$\alpha_\lambda(k) = \frac{(-1)^\lambda I_k k_\lambda \sin(nkl)}{\sqrt{\pi l}(k^2 - k_\lambda^2)}, \quad (60)$$

$$\beta(k, k') = \frac{i}{2\pi} \left[\mathcal{P} \left(\frac{1 - S_c^*(k')S_k}{k' - k} + \frac{S_c^*(k') - S_k}{k' + k} \right) - i\pi(1 + S_c^*(k)S_k)\delta(k' - k) \right], \quad (61)$$

where S_k and I_k are given by equation (A.5) and equation (A.6), respectively. Figure 4 shows the real part of the scattering wave function with $kl = 28.9$. The exact solution (A.4) (solid gray line) is compared with the mode expansion (dashed line) using the expansion coefficients (60) and (61). The first 35 cavity modes were included. The deviations from the exact scattering wave function visible near $x = 0$ can be made arbitrary small by including more terms in the mode expansion.

In order to find the resonances one must solve the eigenvalue equation for $L_{\text{eff}}(k)$. The real space representation of $L_{\text{eff}}(k)$ for our choice of boundary conditions follows upon combination of equations (18) and (52a) (see Appendix B), with the result

$$L_{\text{eff}}(k)\mu(x) = -\frac{d^2}{dx^2}\mu(x) + \delta'(x - 0_-) \left[\mu(0_-) - \frac{1}{k(i + \eta k)} \frac{d}{dx'}\mu(x')\Big|_{x'=0_-} \right], \quad (62)$$

where $\mu(x)$ is an arbitrary resonator state. The range of $L_{\text{eff}}(k)$ within Hilbert space is defined by the resonator functions for which the singular term on the right hand side

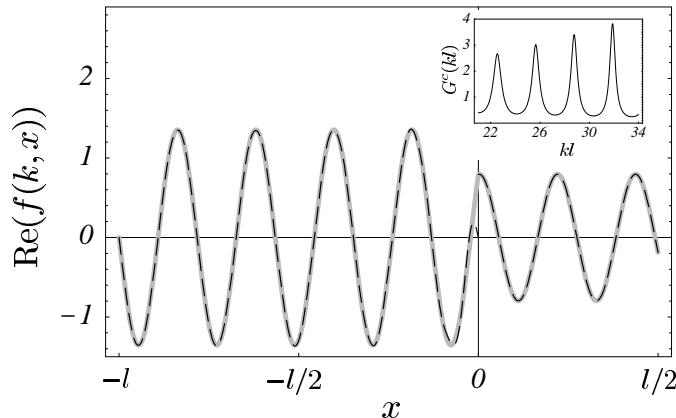


Figure 4. Real part of the scattering wave function with $kl = 28.9$ for a one dimensional optical cavity with a perfectly reflecting mirror at $x = -l$ and a semitransparent mirror at $x = 0$. The mirror transparency is characterized by $\eta = 0.0453$ corresponding to the reflection coefficient $|r(kl = 28.9)|^2 = 0.3$. The solid line is the exact solution, the dashed line represents the mode expansion truncated to the first 35 modes in the cavity region. Inset: Cavity gain factor as function of kl for a range around $kl = 28$.

vanishes. In particular, this holds for the right eigenstates $\xi_j(k, x)$. It follows that these states satisfy the boundary condition

$$\xi_j(k, x) = \frac{1}{k(i + \eta k)} \frac{d}{dx} \xi_j(k, 0_-) \Big|_{x=0_-}, \quad (63)$$

at the semitransparent mirror. There is a discrete set of solutions,

$$\xi_j(k, x) = A_j(k) \sin(\sigma_j(k)(x + L)), \quad (64)$$

with some normalization constant $A_j(k)$. Substitution into equation (63) yields the equation for the eigenvalues $\sigma_j(k)$,

$$\sigma_j(k) \cot(\sigma_j(k)l) = k(i + k\eta). \quad (65)$$

After analytical continuation of the fixed point equation $k = \sigma_j(k)$ into the complex plane we obtain the resonance condition

$$i + \eta k - \cot(kl) = 0, \quad (66)$$

that coincides with the equation for the poles of the S -matrix (cf. equation (A.5)).

To quantify the resonant response of the cavity to external excitations we compute the integrated local density of states, again using the Poisson sum rule,

$$\begin{aligned} \int_{-l}^0 dx \rho(k, x) &= \frac{l|I_k|^2 \sin^2(kl)}{l^2\pi} \sum_{\lambda=1}^{+\infty} \frac{k_\lambda^2}{(k^2 - k_\lambda^2)^2}, \\ &= \frac{l|I_k|^2}{4\pi} \left[1 - \frac{\sin(2kl)}{2kl} \right]. \end{aligned} \quad (67)$$

Combination with the free-space density of states (40) gives the cavity gain factor

$$G^c(k) = \frac{1}{\left[1 - \eta k \sin(2kl) + (\eta k)^2 \sin^2(nkl)\right]}. \quad (68)$$

With increasing kl sharper resonances are found in the cavity gain factor (see figure 4(inset)). The reason is the reduction of the mirror transmission for large kl that, in turn, enhances the lifetime of the cavity resonances.

5. Dielectric disk

In this section we demonstrate our quantization technique for resonators of spatial dimension larger than one. Specifically, we consider a two-dimensional circular dielectric of radius R and refractive index n (see figure 1(c)). The resonator is embedded in free space. We restrict ourselves to TM modes with the electric field polarized in the z -direction. It is convenient to use polar coordinates $\mathbf{r} = (r, \phi)$ below. The dielectric function then reads

$$\epsilon(r) = n^2 \Theta(R - r) + \Theta(r - R). \quad (69)$$

The scattering problem at the resonator can be solved exactly. The exact eigenmodes of Maxwell's equations are summarized in equation (A.7).

To apply our quantization technique we separate system and bath along the boundary of the dielectric: The dielectric disk ($r \leq R_-$) is taken as the cavity, while the free space ($r \geq R_+$) becomes the channel region. For the cavity we assume Dirichlet boundary conditions at $r = R_-$, which implies Neumann conditions at $r = R_+$ for the channel problem. The differential operator resulting from this choice reads

$$L_{\mathcal{Q}\mathcal{Q}}\mu(r, \phi) = -\frac{1}{n^2} \nabla^2 \mu(r, \phi) + \frac{\partial}{\partial r} \left(\frac{1}{r} \delta(r - R_-) \right) \frac{R_-}{n^2} \mu(R_-, \phi), \quad (70a)$$

$$L_{\mathcal{P}\mathcal{P}}\nu(r, \phi) = -\nabla^2 \nu(r, \phi) - \delta(r - R_+) \frac{\partial}{\partial r'} \nu(r', \phi) \Big|_{r'=R_+}, \quad (70b)$$

$$L_{\mathcal{P}\mathcal{Q}}\mu(r, \phi) = \frac{\delta(r - R_+)}{n} \frac{\partial}{\partial r'} \mu(r', \phi) \Big|_{r'=R_-}, \quad (70c)$$

$$L_{\mathcal{Q}\mathcal{P}}\nu(r, \phi) = -\frac{\partial}{\partial r} \left(\frac{1}{r} \delta(r - R_-) \right) \frac{R_-}{n} \nu(R_+, \phi). \quad (70d)$$

Due to the rotational symmetry we can choose the eigenstates to be angular momentum eigenstates.

The eigenmodes $\mu_{m\lambda}$ of the closed cavity are labeled by the angular momentum number m and the radial quantum number λ . They solve the Helmholtz equation

$$\nabla^2 \mu_{m\lambda}(r, \phi) = -n^2 k_{m\lambda}^2 \mu_{m\lambda}(r, \phi), \quad (71)$$

and satisfy the Dirichlet condition $\mu_{m\lambda}(R_-, \phi) = 0$. The normalized eigenstates are given in terms of Bessel functions of the first kind,

$$\mu_{m\lambda}(r, \phi) = \frac{e^{im\phi} J_m(nk_{m\lambda}r)}{\sqrt{\pi} R J_{m+1}(x_{m\lambda})}, \quad (72)$$

with $m = 0, \pm 1, \pm 2, \dots$ and $\lambda = 0, 1, 2, \dots$. The eigenvalues are $k_{m\lambda} = x_{m\lambda}/nR$ where $x_{m\lambda}$ denotes the λ -th zero of $J_m(r)$. In a similar fashion, one determines the eigenstates in the channel region. They can be written in terms of Hankel functions,

$$\nu_m(k, r, \phi) = \sqrt{\frac{k}{8\pi}} e^{im\phi} (H_m^{(2)}(kr) + S_m(k) H_m^{(1)}(kr)), \quad (73)$$

with the diagonal element of the scattering matrix

$$S_m(k) = -\frac{H_m'^{(2)}(kR)}{H_m'^{(1)}(kR)}. \quad (74)$$

The channel states obey the Neumann condition $\left. \frac{\partial}{\partial r} \nu_m(k, r, \phi) \right|_{r=R_+} = 0$.

In addition to the internal frequencies $\omega_{m\lambda} = ck_{m\lambda}$ we need the coupling amplitudes \mathcal{W} and \mathcal{V} to fully determine the system–and–bath Hamiltonian. Combination of equation (70d) with the mode functions (72), (73) and the definitions (16a) and (16b) yields after a short calculation

$$\mathcal{W}_{m\lambda, n}(k) = \frac{-i\sqrt{2k_{m\lambda}}}{\pi k R H_m'^{(1)}(kR)} \delta_{m, n}, \quad (75)$$

$$\mathcal{V}_{m\lambda, n}(k) = \frac{-i\sqrt{2k_{m\lambda}}}{\pi k R H_m'^{(1)}(kR)} \delta_{m, -n}. \quad (76)$$

We note that the resonant amplitude \mathcal{W} couples only cavity and channel modes with the same angular momentum, while the antiresonant amplitude \mathcal{V} couples modes with opposite angular momentum. This feature guarantees angular momentum conservation: The resonant terms $\mathcal{W}_{\lambda m} a_m^\dagger b_m$ and $\mathcal{W}_{\lambda m}^* a_m b_m^\dagger$ account for the creation of a photon with angular momentum m and the simultaneous annihilation of a second photon with the same angular momentum. By contrast, the antiresonant terms, $\mathcal{V}_{\lambda m} a_{m\lambda} b_{-m}$ and $\mathcal{V}_{\lambda m}^* a_{m\lambda} b_{-m}$ describe the simultaneous annihilation or creation of two photons with opposite value of angular momentum. In both cases, the total angular momentum is conserved.

We now turn to the electromagnetic field and the cavity resonances. In the cavity region the exact scattering states $f_m(k)$ can be represented in terms of the cavity modes $u_{m\lambda}$, with the expansion coefficients

$$\alpha_{m\lambda, n}(k) = \sqrt{\frac{k}{2}} \frac{k_{m\lambda} I_{mk} J_m(nkR)}{n(k^2 - k_{m\lambda}^2)} \delta_{m, n}, \quad (77)$$

where I_{mk} is given by equation (A.9). It suffices to compare the radial component of the scattering wave functions. In figure 5 we show the real part of that component for angular momentum $m = 13$ and $kR = 10.5$. The solid gray line is the exact result (A.7) while the dotted and dashed lines represent the system–and–bath expansion using the first 11 and 25 cavity modes, respectively.

The cavity resonances are obtained by solving the eigenvalue problem for $L_{\text{eff}}(k)$. The calculation is presented in Appendix B and yields the resonance condition

$$J_m(nkR) H_m'^{(1)}(kR) - n J_m'(nkR) H_m^{(1)}(kR) = 0, \quad (78)$$

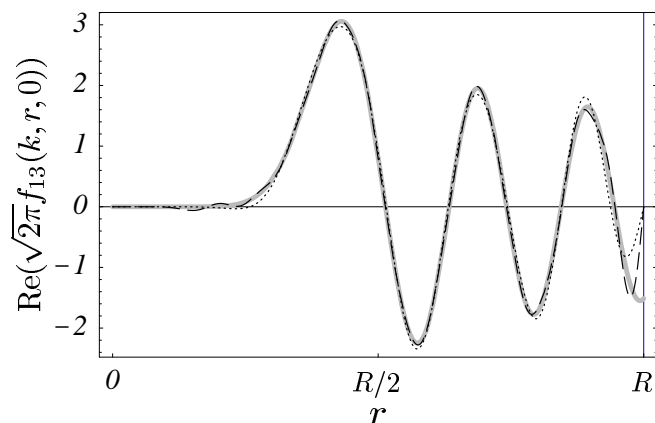


Figure 5. Real part of the radial component of the scattering wave function with angular momentum $m = 13$ and $kR = 10.5$ inside a dielectric disk with radius R and index of refraction $n = 3.3$. The solid gray curve is the exact result. The dotted (dashed) line follows from the mode expansion taking into account the first 11 (25) cavity modes.

which is equivalent to the equation that determines the poles of the S -matrix (cf. equation (A.8)).

Substitution of equation (77) into equation (21) yields the integrated local density of states inside the dielectric disk (see Appendix C),

$$\int_{\text{disk}} d\mathbf{r} \rho(k, \mathbf{r}) = \sum_{m=-\infty}^{+\infty} \frac{kR^2 |I_{mk}|^2}{8n^2} \left(J_m^2(nkR) - J_{m+1}(nkR) J_{m-1}(nkR) \right). \quad (79)$$

Together with the free-space local density of states $\rho_0(k) = k/2\pi$, we obtain the cavity gain factor

$$G^c(k) = \frac{4 (J_m^2(nkR) - J_{m+1}(nkR) J_{m-1}(nkR))}{(\pi nkR)^2 |J_m(nkR) H_m^{(1)}(kR) - n J'_m(nkR) H_m^{(1)}(kR)|^2}, \quad (80)$$

where we used the explicit expression (A.9) for the mode amplitude I_{mk} . The cavity gain factor displays a set of very sharp resonances (see figure 6), corresponding to states with angular momentum $kR < m < nkR$, superimposed over a smooth background due to broad resonances with $m < kR$ [30].

6. Conclusion

In this paper we have derived exact system-and-bath Hamiltonians for a number of optical resonators. Physical observables computed with these Hamiltonian agree with the results obtained by direct scattering methods. It follows that the system-and-bath approach, originally developed as a phenomenological model, can provide an exact quantitative description of optical systems even in the regime of overlapping modes.

On a formal level our quantization method is based on the Feshbach projector technique [21] that has extensively been used in nuclear and condensed matter physics

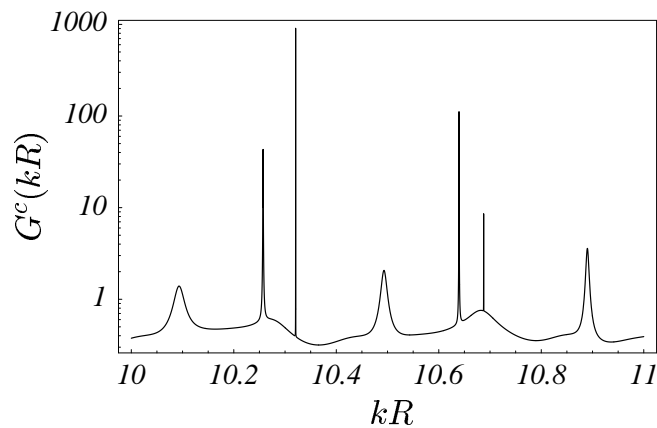


Figure 6. Cavity gain factor as function of kR for a dielectric disk with radius R and index of refraction $n = 3.3$. The sharp resonances correspond to states with angular momentum $10 < m < 18$, very sharp resonances with $m \gg 18$ are not resolved.

[31, 32]. In that areas the method has become a powerful tool for the description of disordered and chaotic media. Statistical theories for such media have been obtained employing a random–matrix assumption for the underlying system Hamiltonian [17]. Our application of the projector technique to the field of quantum optics may lay the ground for a statistical treatment of disordered and wave–chaotic optical media.

Acknowledgments

We thank P. Braun, F. Haake, D. V. Savin, H.-J. Sommers and J. D. Urbina for helpful discussions. This work has been supported in part by an Heisenberg fellowship and by the SFB/TR 12 der Deutschen Forschungsgemeinschaft.

Appendix A. Exact modes of Maxwell’s equations

In this appendix we summarize the exact solutions of Maxwell’s equations for the three systems treated in the paper; for a more detailed derivation we refer to references [27, 29, 30]. The modes–of–the–universe are taken to be scattering states with an incoming wave in only one scattering channel. In the 2d example, this channel is labeled by the angular momentum number m . The scattering states are normalized according to equation (6).

Appendix A.1. One dimensional dielectric cavity

For the dielectric cavity of figure 1(a) the scattering states are given by

$$f(k, x) = \frac{1}{\sqrt{2\pi}} \begin{cases} \frac{I_k}{n} \sin(nk(x+l)) & (-l < x < 0), \\ \exp(-ikx) + S_k \exp(ikx) & (0 < x). \end{cases} \quad (\text{A.1})$$

They satisfy the boundary condition $f(k, -l) = 0$, imposed by the completely reflecting mirror at $x = -l$, and are continuous with continuous derivative for any value of $x > -l$. The single-channel S-matrix and the mode strength amplitude are given, respectively, by

$$S_k = -\frac{n + i \tan(nkl)}{n - i \tan(nkl)}, \quad (\text{A.2})$$

$$I_k = \frac{-2in}{n \cos(nkl) - i \sin(nkl)}. \quad (\text{A.3})$$

Appendix A.2. Cavity with semitransparent mirror

The scattering states for the one dimensional cavity with the semitransparent mirror (Fig. 1(b)) have the form

$$f(k, x) = \frac{1}{\sqrt{2\pi}} \begin{cases} I_k \sin(k(x+l)) & (-l < x < 0), \\ \exp(-ikx) + S_k \exp(ikx) & (0 < x), \end{cases} \quad (\text{A.4})$$

where the scattering matrix S_k and the mode strength amplitude I_k are given by

$$S_k = \frac{i - \eta k + \cot(kl)}{i + \eta k - \cot(kl)}, \quad (\text{A.5})$$

$$I_k = \frac{2i}{(i + k\eta) \sin(kl) - \cos(kl)}. \quad (\text{A.6})$$

Here η specifies the mirror transparency. The modes satisfy $f(k, -l) = 0$ at the perfectly reflecting mirror and are continuous everywhere else. At the semitransparent mirror their derivative has a discontinuity proportional to the mode amplitude, $f'(k, 0_+) - f'(k, 0_-) = -\eta k^2 f(k, 0)$, where the prime denotes differentiation with respect to the position.

Appendix A.3. Dielectric disk

The exact eigenstates for a two dimensional dielectric disk of radius R and refractive index n embedded in empty space read

$$f_m(k, r, \phi) = \sqrt{\frac{k}{8\pi}} e^{-im\phi} \begin{cases} I_{mk} J_m(nkr) & (0 < r < R), \\ H_m^{(2)}(kr) + S_{mk} H_m^{(1)}(kr) & (R < r), \end{cases} \quad (\text{A.7})$$

where m labels angular momentum. The channel with index m is open when k exceeds the channel threshold $k_m = m/nR$. Due to rotational symmetry angular momentum is conserved, and the S-matrix is diagonal in the angular momentum basis

$$S_{mk} = -\frac{H_m^{(2)}(kR) - n[J'_m(nkR)/J_m(nkR)]H_m^{(2)}(kR)}{H_m^{(1)}(kR) - n[J'_m(nkR)/J_m(nkR)]H_m^{(1)}(kR)}. \quad (\text{A.8})$$

The mode strength amplitude takes the form

$$I_{mk} = \frac{4i}{\pi k R \left(J_m(nkR) H_m^{(1)}(kR) - n J'_m(nkR) H_m^{(1)}(kR) \right)}. \quad (\text{A.9})$$

Appendix B. External Green functions

Here we evaluate the action of the non-Hermitian differential operator $L_{\text{eff}}(k)$ on an arbitrary cavity state. According to equation (18) $L_{\text{eff}}(k)$ is the sum of two operators. The first contribution $L_{\mathcal{Q}\mathcal{Q}}$ has already been computed in equations (23a), (43a), (52a) and (70a). The second contribution has the form

$$L_{\mathcal{Q}\mathcal{P}}\mathcal{G}_{\text{ch}}(k)L_{\mathcal{P}\mathcal{Q}}\mu(r, \phi) = L_{\mathcal{Q}\mathcal{P}} \sum_m \int_{k_m}^{\infty} dk' \frac{|\boldsymbol{\nu}_m(k')\rangle\langle\boldsymbol{\nu}_m(k')|}{k^2 - k'^2 + i\epsilon} L_{\mathcal{P}\mathcal{Q}}\mu(r, \phi), \quad (\text{B.1})$$

where \mathcal{G}_{ch} stands for the retarded Green function of the isolated channel region. Below we compute this contribution for the cavities of interest.

Appendix B.1. One dimensional channel

For a one dimensional semi-infinite channel $x \geq 0$ with Dirichlet boundary conditions at $x = 0_+$ we find the retarded Green function from the solutions (29) by contour integration,

$$\begin{aligned} \mathcal{G}_{\text{ch}}(k, x, x') &= \frac{2}{\pi} \int_0^{\infty} dk' \frac{\sin(k'x) \sin(k'x')}{k^2 - k'^2 + i\epsilon} \\ &= \frac{i}{2k} \left(e^{ik|x+x'|} - e^{-ik|x-x'|} \right). \end{aligned} \quad (\text{B.2})$$

Combination with the definitions (23c), (23d) yields the real space representation of $L_{\text{eff}}(k)$. The relevant derivatives have to be done with care as the limits $x \rightarrow 0$ and $x' \rightarrow 0$ must be taken independently. The result takes the form

$$L_{\mathcal{Q}\mathcal{P}}\mathcal{G}_{\text{ch}}(k)L_{\mathcal{P}\mathcal{Q}}\mu(x) = -\frac{ik\delta(x-0_-)}{n^2}\mu(0_-). \quad (\text{B.3})$$

Together with equation (23a) we arrive at the result (33) for $L_{\text{eff}}(k)$.

In a similar fashion we evaluate the retarded Green function for the isolated channel problem with Neumann conditions at $x = 0_+$. Using the solutions (45) we obtain in this case

$$\begin{aligned} \mathcal{G}_{\text{ch}}(k, x, x') &= \frac{2}{\pi} \int_0^{\infty} dk' \frac{\cos(k'x) \cos(k'x')}{k^2 - k'^2 + i\epsilon} \\ &= -\frac{i}{2k} \left(e^{ik|x+x'|} + e^{-ik|x-x'|} \right). \end{aligned} \quad (\text{B.4})$$

Combination with the real space representation (43c) and (43d) of $L_{\mathcal{P}\mathcal{Q}}$ and $L_{\mathcal{Q}\mathcal{P}}$, respectively, yields

$$L_{\mathcal{Q}\mathcal{P}}\mathcal{G}_{\text{ch}}(k)L_{\mathcal{P}\mathcal{Q}}\mu(x) = \frac{i\delta'(x-0_-)}{n^2k} \frac{d}{dx'}\mu(x') \Big|_{x'=0_-}. \quad (\text{B.5})$$

Combinations of equations (18), (43a), and (B.5) yields $L_{\text{eff}}(k)$ given in equation (49).

Appendix B.2. Channel with semitransparent mirror

The semitransparent mirror has width d and refractive index n . In the limit $d \rightarrow 0$, $n \rightarrow \infty$ with $n^2 d = \eta$ fixed, the retarded Green function can be expressed in terms of an integral over products of the scattering states (58),

$$\mathcal{G}_{\text{ch}}(k, x, x') = \frac{1}{2\pi} \int_{-\infty}^{\infty} dk' \frac{e^{ik'(x-x')} + S_c(k')e^{ik'(x+x')}}{k^2 - k'^2 + i\epsilon}. \quad (\text{B.6})$$

The integral can be done by contour integration. Using the unitarity of $S_c(k)$ and taking into account that $S_c(k)$ is analytic in the upper half of the complex plane, equation (B.6) reduces to

$$\mathcal{G}_{\text{ch}}(k, x, x') = -\frac{i}{2k} \left(e^{ik|x-x'|} + S_c(k)e^{ik|x+x'|} \right). \quad (\text{B.7})$$

Combination with the definitions (52c) and (52d) yields

$$L_{\mathcal{QP}}\mathcal{G}_{\text{ch}}(k)L_{\mathcal{PQ}}\mu(x) = -\frac{\delta'(x-0_-)}{k(i+\eta k)} \frac{d}{dx'}\mu(x') \Big|_{x'=0_-}. \quad (\text{B.8})$$

Equations (52a), (B.8) along with equation (18) yield equation (62).

Appendix B.3. Angular momentum channels

The retarded Green function for the two-dimensional Helmholtz equation with Neumann boundary conditions along a disk of radius R , has the form

$$\begin{aligned} \mathcal{G}_{\text{ch}}(k, r', \phi', r, \phi) &= -\frac{i}{2\pi} \sum_{-\infty}^{+\infty} e^{im(\phi-\phi')} \frac{H_m^{(1)}(kr_>)}{H_m^{(1)}(kR)} \\ &\times \left(H_m^{(2)}(kr_<)H_m^{(1)}(kR) - H_m^{(2)}(kR)H_m^{(1)}(kr_<) \right), \end{aligned} \quad (\text{B.9})$$

where $r_<$ ($r_>$) stands for the smaller (larger) of r and r' . Substitution of the definitions (70c) and (70d) yields

$$\begin{aligned} L_{\mathcal{QP}}\mathcal{G}_{\text{ch}}(k)L_{\mathcal{PQ}}\mu(r, \phi) &= -\frac{R}{2n^2\pi} \frac{\partial}{\partial r} \left(\frac{1}{r} \delta(r-R_-) \right) \\ &\times \sum_{m=-\infty}^{+\infty} \int_0^{2\pi} d\phi' e^{im(\phi-\phi')} \frac{H_m^{(1)}(kR)}{kH_m^{(1)}(kR)} \frac{\partial}{\partial r''} \mu(r'', \phi') \Big|_{r''=R_-}. \end{aligned} \quad (\text{B.10})$$

Combination with equations (18) and (70a) shows that $L_{\text{eff}}(k)$ acts on an arbitrary resonator state $\mu(r, \phi)$ like

$$\begin{aligned} L_{\text{eff}}(k)\mu(r, \phi) &= -\frac{1}{n^2} \nabla^2 \mu(r, \phi) + \frac{R}{n^2} \frac{\partial}{\partial r} \left(\frac{1}{r} \delta(r-R_-) \right) \left[\mu(R_-, \phi) \right. \\ &\left. - \frac{1}{2\pi} \sum_{m=-\infty}^{+\infty} \int_0^{2\pi} d\phi' e^{im(\phi-\phi')} \frac{H_m^{(1)}(kR)}{kH_m^{(1)}(kR)} \frac{\partial}{\partial r''} \mu(r'', \phi') \Big|_{r''=R_-} \right]. \end{aligned} \quad (\text{B.11})$$

Conservation of angular momentum and the requirement that the singular terms must vanish for the right eigenstates $\xi_{mj}(k, r, \phi)$ yield the boundary condition

$$\xi_{mj}(k, R_-, \phi) = \frac{H_m^{(1)}(kR)}{kH_m^{(1)}(kR)} \frac{\partial}{\partial r''} \xi_{mj}(k, r'', \phi) \Big|_{r''=R_-}. \quad (\text{B.12})$$

There is a discrete set of solutions

$$\xi_{mj}(k, r, \phi) = A_{mj}(k)e^{im\phi}J_m(n\sigma_{mj}(k)r), \quad (\text{B.13})$$

with normalization constants $A_{mj}(k)$. Substitution into equation (B.12) yields the equation for the eigenvalues

$$kJ_m(n\sigma_{mj}(k)R)H_m^{(1)}(kR) - n\sigma_{mj}(k)J_m'(n\sigma_{mj}(k)R)H_m^{(1)}(kR) = 0. \quad (\text{B.14})$$

Combination with the fixed point equation $k = \sigma_{mj}(k)$ finally gives the resonance condition (78).

Appendix C. Local density of states inside the dielectric disk

Here we determine the density of states inside a dielectric disk with radius R and refractive index n . We start from equation (21). Using the coefficients (77), we obtain

$$\int_{\text{disk}} d\mathbf{r} \rho(k, \mathbf{r}) = \sum_{m=-\infty}^{+\infty} \frac{k|I_{mk}|^2}{2n^2} J_m^2(nkR) \sum_{\lambda=1}^{\infty} \frac{k_{m\lambda}^2}{(k^2 - k_{m\lambda}^2)^2}. \quad (\text{C.1})$$

We concentrate on the evaluation of the last sum on the right hand side. It can be written as a derivative

$$\sum_{\lambda=1}^{\infty} \frac{k_{m\lambda}^2}{(k^2 - k_{m\lambda}^2)^2} = -\frac{1}{2} \frac{\partial}{\partial \alpha} \sum_{\lambda=1}^{\infty} \frac{1}{(k^2 - \alpha^2 k_{m\lambda}^2)} \Big|_{\alpha=1}. \quad (\text{C.2})$$

The right hand side can be simplified by noticing that $nRk_{m\lambda} = x_{m\lambda}$ is the λ -th zero of the Bessel function $J_m(x)$. The sum on the right hand side can then be identify as the trace of the Green function for the radial part of the Helmholtz equation, in a dielectric disk with Dirichlet conditions on the disk perimeter. Equation (C.2) becomes

$$\sum_{\lambda=1}^{\infty} \frac{k_{m\lambda}^2}{(k^2 - k_{m\lambda}^2)^2} = -\frac{1}{2} \frac{\partial}{\partial \alpha} \int_0^R dr r \mathcal{G}_{\text{disk}}(k/\alpha, r, r) \Big|_{\alpha=1}. \quad (\text{C.3})$$

The disk Green function can be found by standard methods [33] and is given by

$$\begin{aligned} \mathcal{G}_{\text{disk}}(k/\alpha, r', r) &= \frac{i\pi}{4J_m(nkR/\alpha)} J_m(nkr_{<}/\alpha) \\ &\times (J_m(nkR/\alpha) Y_m(nkr_{>}/\alpha) - Y_m(nkR/\alpha) J_m(nkr_{>}/\alpha)), \end{aligned} \quad (\text{C.4})$$

where Y_m is a Bessel function of the second kind and $r_{<}$ ($r_{>}$) the smaller (larger) of r and r' . The problem then reduces to the evaluation of the integral in equation (C.3). Using the relations

$$\int_0^R dr r J_m^2(kr) = \frac{R^2}{2} (J_m^2(kR) - J_{m+1}(kR)J_{m-1}(kR)), \quad (\text{C.5})$$

$$\begin{aligned} \int_0^R dr r J_m(kr) Y_m(kr) &= \frac{R^2}{2} (J_m(kR) Y_m(kR) - \frac{1}{2} J_{m+1}(kR) Y_{m-1}(kR) \\ &\quad - \frac{1}{2} J_{m-1}(kR) Y_{m+1}(kR)), \end{aligned} \quad (\text{C.6})$$

we find after some straightforward manipulations the result

$$\int_0^R dr r \mathcal{G}_{\text{disk}}(k/\alpha, r, r) = \frac{\alpha R J'_m(kR/\alpha)}{2k J_m(kR/\alpha)}. \quad (\text{C.7})$$

Substitution into equation (C.3) yields

$$\sum_{\lambda=1}^{\infty} \frac{k_{m\lambda}^2}{(k^2 - k_{m\lambda}^2)^2} = \frac{R^2}{4J_m^2(nkR)} \left(J_m^2(nkR) - J_{m+1}(nkR)J_{m-1}(nkR) \right). \quad (\text{C.8})$$

After substitution into equation (C.1) one arrives at the integrated density of states (79).

References

- [1] Senitzky I R 1959 *Phys. Rev.* **119** 670
- [2] Senitzky I R 1960 *Phys. Rev.* **124** 642
- [3] Gardiner C W and Zoller P 2000 *Quantum Noise* (Berlin: Springer)
- [4] Hackenbroich G, Viviescas C and Haake F 2002 *Phys. Rev. Lett.* **89** 083902
- [5] Viviescas C and Hackenbroich G 2003 *Phys. Rev. A* **67** 013805
- [6] Gruner T and Welsch D -G 1996 *Phys. Rev. A* **54** 1661
- [7] Dalton B J, Barnett S M and Knight P L 1999 *J. Mod. Opt.* **46** 1315
- [8] Dutra S M and Nienhuis G 2000 *Phys. Rev. A* **62** 063805
- [9] Hamel W A and Woerdman J P 1989 *Phys. Rev. A* **40** 2785
- [10] van Eijkelenborg M A, Lindberg Å M, Thijssen M S and Woerdman J P 1996 *Phys. Rev. Lett.* **77** 4314
- [11] Lindberg Å M, van Eijkelenborg M A, Joosten K, Nienhuis G and Woerdman J P 1998 *Phys. Rev. A* **57** 3036
- [12] Frolov S V, Vardeny Z V, Yoshino K, Zakhidov A and Baughman R H *Phys. Rev. B* **59** R5284
- [13] Cao H, Zhao Y G, Ho S T, Seelig E W, Wang Q H and Chang R P H 1999 *Phys. Rev. Lett.* **82** 2278
- [14] Cao H, Ling Y, Xu J Y, Cao C Q and Kumar P 2001 *Phys. Rev. Lett.* **86** 4524
- [15] Cao H 2003 *Wave Random Media* **13** R1
- [16] Lang R, Scully M O and Lamb Jr W E 1973 *Phys. Rev. A* **7** 1788
- [17] Guhr T, Müller-Groeling A and Weidenmüller H A 1998 *Phys. Rep.* **299** 189
- [18] Hackenbroich G, Viviescas C and Haake F 2003 *Phys. Rev. A* **68** 063805
- [19] Glauber R J and Lewenstein M 1991 *Phys. Rev. A* **43** 467
- [20] Knöll L, Vogel W and Welsch D -G 1991 *Phys. Rev. A* **43** 543
- [21] Feshbach H 1962 *Ann. Phys.* **19** 287
- [22] Savin D V, Sokolov V V and Sommers H -J 2003 *Phys. Rev. E* **67** 026215
- [23] Cohen-Tannoudji C, Dupont-Roc J and Grynberg G 1992 *Atom-Photon Interactions: Basic Processes and Applications* (New York: Wiley)
- [24] Kapur P L and Peierls R 1938 *Proc. Roy. Soc. Lond. A* **166** 277
- [25] Kukulin V I, Krasnopol'sky V M and Horáček J 1989 *Theory of Resonances* (London: Kluwer Academic Publishers)
- [26] de Carvalho C A A and Nussenzveig H M 2002 *Phys. Rep.* **364** 83
- [27] Ujihara K 1975 *Phys. Rev. A* **12** 148
- [28] Barnett S M and Radmore P M 1988 *Opt. Commun.* **68** 364
- [29] Ley M and Loudon R 1987 *J. Mod. Opt.* **34** 227
- [30] Hentschel M and Richter K 2002 *Phys. Rev. E* **66** 056207
- [31] Mahaux C and Weidenmüller H A 1969 *Shell-Model Approach to Nuclear Reactions* (Amsterdam: North-Holland)

[32] Dittes F M 2000 *Phys. Rep.* **339** 215

[33] Jackson J D 1975 *Classical Electrodynamics* (New York: Wiley)